

Frequency Discriminator for the Fine Dust Sensor

Sun Eui Park¹, Ju Yeop Kim, Han Gi Park, Joo Eun Bang, Yu Hwan Shin, and Jae Hyouk Choi^a

Department of Electrical Engineering, Korea Advanced Institute of Science and Technology

E-mail: ¹suneui@kaist.ac.kr

Abstract – This work presents a delay-locked-loop (DLL)-based frequency discriminator for a fine dust sensor. Detecting the frequency variations of MEMS resonator according to the fine dust concentration, the proposed frequency discriminator provides digital codes which represents the frequency variations. Since the proposed frequency discriminator is based on the CMOS process, it achieved extremely small area of 0.18 mm² and low power of 12 mW, which facilitates the integration into portable device. The proposed DLL-based frequency discriminator covers the input frequency range of 1890 to 2486 MHz with a resolution of 144 kHz, thus it can discriminate input frequencies with 4111 steps. Additionally, to increase the PVT robustness, it used K_{VCDL} compensation technique.

Keywords—Delay-Locked Loop(DLL), Fine dust sensor, Frequency discriminator

I. INTRODUCTION

Increasing concentration of fine dust is a serious environmental problem these days since it causes respiratory diseases. The problem becomes worse as the industry progresses. Fine dust is tiny dust whose diameter of a particle is smaller than 10um. Then, it cannot be filtered by human organs. Therefore, people with respiratory diseases should avoid going out when its concentration is high. To measure the concentration of fine dust, optical elements are the popular method for the fine dust sensor. However, it has poor accuracy when it detects particles smaller than the wavelength of light [1], and also, according to the direction of light refraction, its accuracy could be worse.

To increase the sensor’s reliability, system-on-chip (SoC) based smart integrated circuit (IC) can be an alternative solution. SoC based smart IC consists of detection particles such as MEMS resonators [2] – [4] and the information from the particle is dealt in SoC board. Thanks to high interactivity of a SoC, it has area and cost-efficient characteristics. In this work, we only focused on SoC part, and we assumed MEMS resonators whose frequency is varied with mass exists at the front part of the SoC. Figure 1 shows the MEMS resonators we assumed. When the number

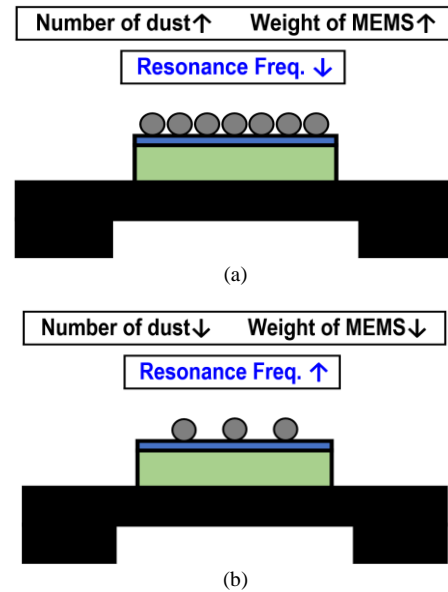


Fig. 1. Operations of MEMS resonators for the fine dust detection in two cases when (a) the number of the fine dust increases and (b) the number of the fine dust decreases.

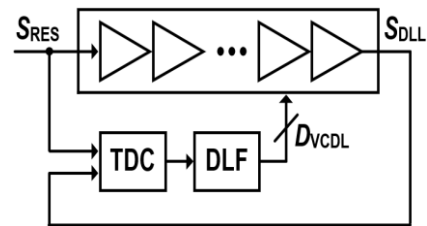


Fig. 2. Basic architecture of a digital DLL.

of dust increases, which means the concentration of the dust is high, the weight of MEMS resonator increases, then, resonance frequency decreases. In similar way, when the number of dust decreases, the weight of MEMS resonator decreases, then, resonance frequency increases. Then, the following SoC part which is the proposed delay-locked-loop-based frequency discriminator detects the frequency changes in the resonator.

The rest of this paper is organized as follows. Section II presents the implementation of the proposed delay-locked-loop (DLL)-based frequency discriminator. Section III shows the results and discussion. Section IV provides conclusions.

a. Corresponding author; jaehyouk@kaist.ac.kr

Manuscript Received May. 06, 2021, Revised Jun. 03, 2021, Accepted Jun. 03, 2021

This is an Open Access article distributed under the terms of the Creative Commons Attribution Non-Commercial License (<http://creativecommons.org/licenses/bync/3.0>) which permits unrestricted non-commercial use, distribution, and reproduction in any medium, provided the original work is properly cited.

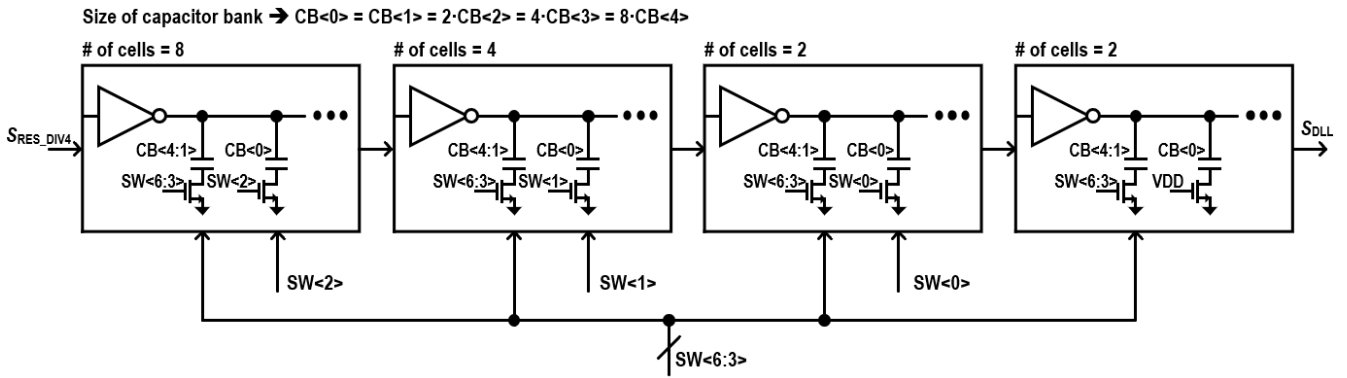


Fig. 5. Implementation of coarse delay cells.

when coarse delay cell's codes increase. By doing so, coarse delay cells increase cover delay range of the fine delay cells.

The operations of the proposed frequency discriminator are as follows. If the frequency of the input signal increases, which means that the fine dust concentration decreases, the 1-bit TDC detects that the delay of the DLL is longer than the period of the input signal, S_{RES_DIV4} . Then, according to the 1-bit TDC's output, the digital code of the 12-bit ACC is updated. The accumulator's digital value is transferred as an analog value through 4-bit RDAC and 2nd-RC filter, which controls the delay of the delay cells to the direction of removing the delay offset between the DLL and the input clock. As a result, after the delay is locked to the appropriate value according to the input signal's frequency, we can get the dust concentration by simply reading the accumulator's digital code number. 12-bit DSM was used to increase the resolution of the fine delay cells, and 2nd-order RC filter was used to reduce large ripples from the DSM operation which can interfere the performance of the proposed frequency discriminator. ACC_WRITE<11:0> was set manually to set D_{VCDL} initially for the convenient measurement. Divide by 4 divider and divide by 1250 divider are used to generate timing signals for the 7b-ACC, 12b-ACC, and 12b 2nd DSM, and unity-gain buffer is used to convert accumulator's digital value to analog value.

C. Implementation of coarse delay cells

Figure 5 shows the implementation of coarse delay cells. It consists of 16 inverter-based delay cells. Among 7-bit of the coarse delay code, 4-bits of MSB, SW<6:3> is connected to all 16 delay cells. To reduce the design burden from parasitic capacitance, 3-bits of LSB are controlled by the number of delay cells to be connected, i.e., SW<2>, SW<1>, and SW<0> are connected to 8 delay cells, 4 delay cells, and 2 delay cells, respectively. Each switch is connected to the gate of NMOS switches which is connected in series with the load capacitance of CB<4:0>, where the capacitor bank has binary sizing, i.e., $CB<1> = 2 \cdot CB<2> = 4 \cdot CB<3> = 16 \cdot CB<4>$. CB<0> has the same size of CB<1> since CB<0> is connected to only part of delay cells while CB<1> is connected to all 16 delay cells. At the right side two delay cells' CB<0>'s switches' gates are connected to VDD to increase the linearity of total bank.

III. RESULTS AND DISCUSSION

Figure 6 shows the micrograph of the proposed DLL-based frequency discriminator. Fabricated in a 180-nm CMOS technology, it used an active area of 0.18 mm². Four same frequency discriminators are merged into same die to increase the accuracy of measurements, and for the measurement, we only used one of four frequency discriminators. Figure 7 and 8 show the measured output DLL codes which represent input frequency changes. The code is the output of 12b ACC, D_{VCDL} , according to the input clock S_{RES} 's frequency, f_{RES} . In Fig. 7, the coarse delay cell's control code, SW<6:0> is 111111₂, which means it has longest delay. Then, the fine delay cells cover from 1890.0 to 2030.5 MHz. During the range, the DLL output code linearly decreases as the input resonance frequency of MEMS resonator, f_{RES} , increases. Since the fine delay cells covers only 200 ps, the proposed DLL can achieve extremely fine steps which are smaller than 150 fs. When the fine delay cell's control codes are full, the coarse delay cell's control code increases to compensate the fine delay cells. In Fig. 8, the coarse delay cell's control code, SW<6:0> is 000000₂, which means it has shortest delay. Then, the fine delay cells cover from 2270.0 to 2485.5 MHz. Similarly, the case in Fig. 7, during the range, the DLL output code linearly decreases as the input resonance frequency of MEMS resonator, f_{RES} , increases.

Figure 9 shows transient simulation results which is from a post-layout simulation. It is an output of unity-gain buffer which is connected to the output of RDAC, V_{TUNE} . The highest voltage of RDAC is 1.8-V and the lowest voltage of

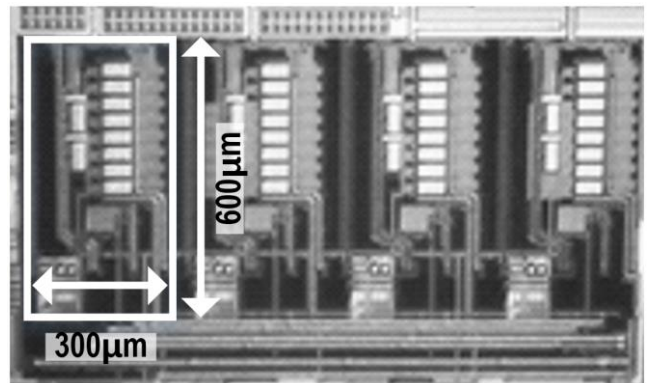


Fig. 6. Micrograph.

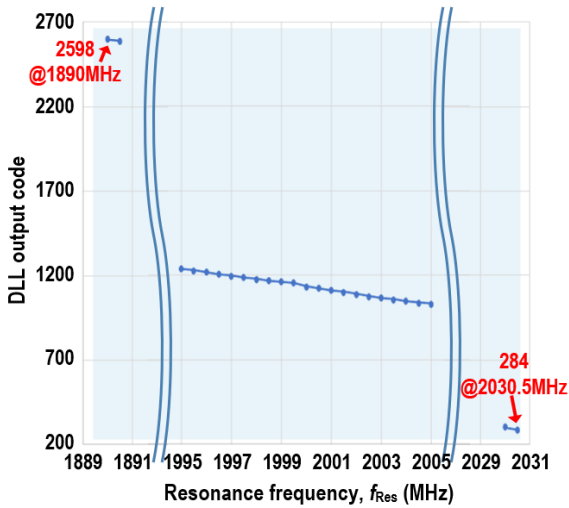


Fig. 7. Measured 12b ACC's output code, D_{VCDL} , according to the input clock S_{RES} 's frequency, f_{RES} , when the coarse delay cell's control code, $SW<6:0>$ is 111111₂.

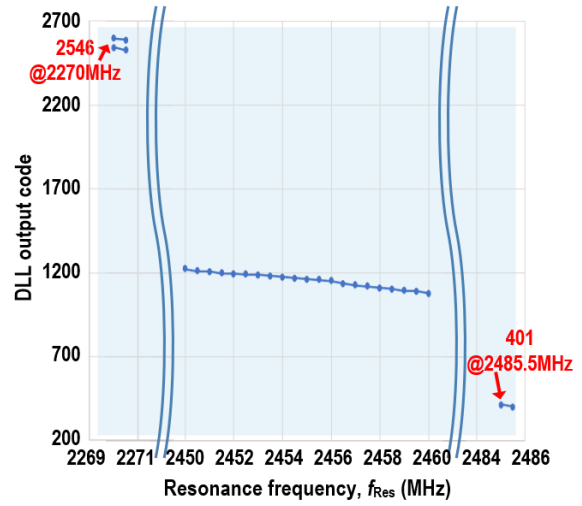


Fig. 8. Measured 12b ACC's output code, D_{VCDL} , according to the input clock S_{RES} 's frequency, f_{RES} , when the coarse delay cell's control code, $SW<6:0>$ is 000000₂.

RDAC is 0 since the 1.8-V supply was used for the implementation of the proposed frequency discriminator. Then, since the fine control code is 12-bit, the control voltage of fine delay cells, V_{TUNE} , is changed of 0.5 mV per 1-bit. In Fig. 9, first decreases in 10 codes is the process of initial locking. After 100us, the input frequency decreases with 200 kHz steps at 250 us, 350 us, 600 us, and 700 us. At the 480us, the input frequency decreases with 400 kHz steps. Through this, we can also discriminate input frequency with an analog method.

Table I shows the summary of target values and measurement results. Performance metrics are categorized with 5 factors, which are input frequency, output frequency, tuning range, bit number of D_{VCDL} , and the resolution. As echoing other measurement results which are shown in previous figures, the proposed DLL-based frequency discriminator covers input frequency range of 1890 to 2486 MHz, output frequency range of 473 to 621, which is the divided version of the input frequency. The tuning range is 27.06 % which is approximately 10 % wider than the target value. The bit number of D_{VCDL} is 12, and the resolution of D_{VCDL} is 36 kHz.

IV. CONCLUSION

The proposed frequency discriminator was implemented with a simple digital DLL architecture. Except delay lines, other blocks are all synthesized, thus, it achieved extremely small area. To increase the resolution of delay cells, 2nd order DSM was used, and for the linearity, K_{VCDL} compensation technique was used. The proposed frequency discriminator in 180-nm CMOS process consumes only 0.18 mm² area and 12 mW of power, where the delay lines consumes 9.5 mW, the digital blocks consumes 2 mW, the RDAC consumes 0.5 mW. Thanks to the high interactivity and low-power architecture, which can reduce the battery size of the sensor, the proposed frequency discriminator is a good candidate for the fine dust sensor market.

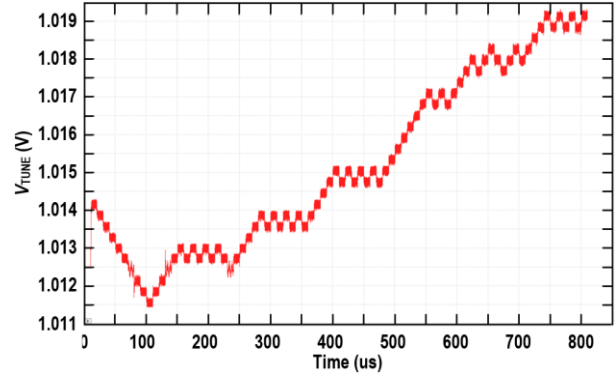


Fig. 9. Transient simulation of V_{TUNE} according to the input frequency changes; input frequency decreases with 200 kHz steps at 100us, 350 us, 600 us, 700us, and 400 kHz steps at 480 us.

TABLE I. The desired specifications and simulation results

Perform. metrics	Target Value	Measurement results
Input frequency (f_{RES})	2000 to 2400 MHz	1890 to 2486 MHz
Output frequency (f_{DLL})	500 to 600 MHz	473 to 621 MHz
Tuning range	18 % <	27.06 %
Bit number of D_{VCDL}	12	12
Resolution	< 50 kHz	36 kHz

ACKNOWLEDGEMENT

This work was supported by Industrial Technology Innovation Program of the Ministry of Trade, Industry & Energy (10080611), and in part by National R&D Program through the National Research Foundation of Korea (NRF) funded by Ministry of Science and ICT

(2020M3H2A1078045), and the chip fabrication was supported by the IC Design Education Center.

REFERENCES

- [1] Choi, J-S., and Park W-T, "MEMS particle sensor based on resonant frequency shifting" *Micro and Nano Syst Lett*, vol. 8, no. 17, Oct. 2020.
- [2] S. B. Paril, V. Chu, and J.P. Conde, "Mass Sensing using an Amorphous Silicon MEMS resonator," *Procedia Chemistry*, vol. 1, no. 1, pp. 1063–1066, Apr. 2009.
- [3] J. Lu *et al.*, "Piezoelectric MEMS devices and its application as bio-chemical sensors," *The 8th Annual IEEE International Conference on Nano/Micro Engineered and Molecular Systems*, 2013, pp. 163-166.
- [4] M. Konno *et al.*, "Novel MEMS oscillator using in-plane disk resonator with sensing platform and its mass sensing characteristics," *2011 16th International Solid-State Sensors, Actuators and Microsystems Conference*, 2011, pp. 518-521.
- [5] Razavi, *RF Microelectronics*. Englewood Cliffs, NJ: Prentice-Hall, 1998.
- [6] J. Lee, S. Choi, Y. Cho, and J. Choi, "Linearly Frequency-Tunable and Low-Phase noise ring VCO using varactors with optimally-spaced bias voltages", *Electronics Lett.*, Jan. 2018.



Sun Eui Park (Student Member, IEEE) was born in Seoul, South Korea, in 1994. She received the B.S. and M.S. degrees in electrical engineering from the Ulsan National Institute of Science and Technology (UNIST), Ulsan, Korea, in 2017 and 2020, respectively. She is currently pursuing the Ph.D. degree with the Korea Advanced Institute of Science and Technology (KAIST), Daejeon,

Korea. Her research interests include analog, mixed-signal IC designs, especially low-power and low-jitter clock generation circuits.



Ju Yeop Kim (Student Member, IEEE) was born in Changwon, South Korea, in 1994. He received the B.S. and M.S. degrees in electrical engineering from the Ulsan National Institute of Science and Technology (UNIST), Ulsan, Korea, in 2017 and 2020, respectively. He is currently pursuing the Ph.D. degree with the Korea Advanced Institute of Science and Technology (KAIST), Daejeon,

Korea. His current research interests include CMOS analog/mixed IC designs, especially millimeter-wave clock/frequency generation systems.



Han Gi Park (S'19) was born in Anseong, South Korea, in 1997. He received the B.S. degree (*summa cum laude*) in electrical engineering from the Ulsan National Institute of Science and Technology (UNIST), Ulsan, South Korea, in 2019. He is currently pursuing the M.S/Ph.D. degree with the Korea Advanced Institute of Science and Technology (KAIST), Daejeon, South Korea.

His research interests include CMOS analog/mixed integrated circuit (IC) designs, especially high-speed clock/frequency generation systems.



Joo Eun Bang (S'18) was born in Busan, South Korea, in 1995. She received the B.S. and M.S. degrees in electrical engineering from the Ulsan National Institute of Science and Technology (UNIST), Ulsan, South Korea, in 2018 and 2020, respectively. She is currently pursuing the Ph.D. degree with the Korea Advanced Institute of Science and Technology (KAIST),

Daejeon, South Korea. Her current research interests include low-power and high-performance analog, mixed-signal, and RF integrated circuits for emerging wireless/wired standards.



Yu Hwan Shin was born in Geoje, South Korea, in 1999. He received the B.S. degree in electrical engineering from the Korea Advanced Institute of Science and Technology (KAIST), Daejeon, South Korea, in 2021. He is currently pursuing the M.S. degree with the Korea Advanced Institute of Science and Technology (KAIST), Daejeon, South Korea.

His research interests include CMOS analog/mixed integrated circuit (IC) designs, especially high-speed clock/frequency generation systems.



Jae Hyouk Choi (Senior Member, IEEE) was born in Seoul, South Korea, in 1980. He received the B.S. degree (*summa cum laude*) in electrical engineering from Seoul National University, Seoul, in 2003 and the M.S. and Ph.D. degrees in electrical and computer engineering from the Georgia Institute of Technology, Atlanta, GA, USA, in 2008 and 2010, respectively.

From 2010 to 2011, he was with Qualcomm, Inc., San Diego, CA, USA, where he was involved in designing multi-standard cellular transceivers. In 2012, he joined the Ulsan National Institute of Science and Technology (UNIST),

Ulsan, South Korea, as a Faculty Member. Since 2019, he has been an Associate Professor with the Korea Advanced Institute of Science and Technology (KAIST), Daejeon, South Korea. His research interests include low-power and high-performance analog, mixed-signal, and RF integrated circuits for emerging wireless/wired standards.

Dr. Choi has been a TPC Member of the IEEE International Solid-State Circuits Conference (ISSCC) since 2017 and the IEEE European Solid-State Circuits Conference (ESSCIRC) since 2016. He was the Country Representative of South Korea for the ISSCC Far-East Region in 2018. He has been a Distinguished Lecturer (DL) of the Solid-State Circuits Society (SSCS) since 2020.